Relaxation of coherent states in a two-qubit NMR quadrupole system

R. S. Sarthour,[1] E. R. deAzevedo,[2] F. A. Bonk,[2] E. L. G. Vidoto,[2] T. J. Bonagamba,[2] A. P. Guimarães,[1] J. C. C. Freitas,[3] and I. S. Oliveira[1]

[1]*Centro Brasileiro de Pesquisas Físicas, Rua Dr. Xavier Sigaud 150, Rio de Janeiro 22290-180, Brazil*

[2]*Instituto de Física de São Carlos, Universidade de São Paulo, São Carlos, P.O. Box 369, São Paulo 13560-970, Brazil*

[3]*Departamento de Física, Universidade Federal do Espírito Santo, Vitória, Espírito Santo 29060-900, Brazil*

(Received 19 March 2003; published 22 August 2003)

We report a detailed study of the longitudinal relaxation of several coherent states on the nuclear-magnetic-resonance (NMR) two-qubit quadrupole system, ^{23}Na (spin 3/2) in a lyotropic liquid-crystal system at room temperature. Relaxation of *pseudopure* states, simulated *pseudo-Bell* states and *Hadamard* states were investigated. The coherence of superposition states was verified by applying the respective quantum ''reading'' operators and comparing the recovered state with the original one. The degree of recovery varies between $\approx 70\%$ and $\approx 100\%$, depending on the time length of the gate, as compared to relaxation times. Spin-lattice relaxation results follow a recently proposed multiexponential model that includes mixed magnetic dipolar and electric quadrupolar interactions. Relaxation curves are governed by initial conditions, and from the experimental curves individual transition rates are derived. The transverse relaxation time constant T_2 is found not to depend on the initial distribution of populations. This is a systematic study of relaxation in the context of NMR quantum computing.

DOI: 10.1103/PhysRevA.68.022311 PACS number(s): 03.67.Lx, 33.25.+k, 76.60.−k

I. INTRODUCTION

Nuclear magnetic resonance (NMR) is to the present date the main experimental technique through which quantum logic gates and full routines have been implemented in several spin-1/2 systems. In spite of recent claims [1] that NMR experiments may not have produced *provable* entanglement phenomena, reported implementations of algorithms by NMR include the following: Deutsch-Josza [2], Grover search [3,4], Shor factorization [5], Brassard teleportation [6], besides simulations of quantum systems [7,8] protocols for generating and reading entangled states [9], etc. This is an impressive achievement, far beyond what any other technique could reach, so far. However, there is a general feeling among the quantum information community that, although NMR is likely to continue for the time being the main technique for testing systems with a small number of qubits, unless signal detection innovations break through, its role in an eventual technological future of quantum computers is very fuzzy, at the best. Nevertheless, there are possibilities that have not been fully explored, which may improve NMR performance in quantum computing applications, such as the use of quadrupole nuclei. Implementation of pseudopure states and logic gates in a four-level two-qubit ^{23}Na and ^{7}Li ($I=3/2$) systems using selective radio-frequency pulses over *equilibrium spectra* has been reported in Refs. [10,11]. In such systems, a nucleus with spin I and electric quadrupole moment Q interacts with a static magnetic field and an axially symmetric electric-field gradient according to [12]

$$\mathcal{H}=-\hbar\omega_L I_z+\hbar\omega_Q[3I_z^2-I^2], \tag{1}$$

where ω_L and ω_Q are, respectively, the Larmor and quadrupole frequencies. For $I=3/2$, this Hamiltonian yields a four-level system with unequal energy spacing, to which one can assign logical labels $|00\rangle$, $|01\rangle$, $|10\rangle$, and $|11\rangle$, corresponding to spins states $|+3/2\rangle$, $|+1/2\rangle$, $|-1/2\rangle$, and $|-3/2\rangle$, respectively. Selective excitation can be achieved if $\omega_L \gg \omega_Q \gg \omega_1$, where ω_1 is the radiofrequency intensity [13,14].

In comparing a spin-3/2 (two-qubit) system to the rather more usual two-spin-1/2 one (such as ^{1}H and ^{13}C in chloroform), there are a few remarks worth making.

(1) The number of qubits per nucleus, N, is bigger in quadrupole systems.

(2) Quadrupolar splittings are usually many orders of magnitude larger than J couplings and therefore spectral resolution is better ($\omega_Q/2\pi \approx 1-100$ kHz, whereas $2\pi J/\hbar \approx 10-300$ Hz).

(3) The free evolution of quadrupole spins goes mainly under the propagator $\exp(-3i\omega_Q t I_z^2)$, whereas in the case of spins 1/2 it goes as $\exp(-i2\pi J t I_{1z} I_{2z}/\hbar)$.

(4) Whereas pseudopure states in a two $I=1/2$ system, due to small J coupling, must be obtained through some sort of averaging [15], in a $I=3/2$ system this is achieved with one single sequence of pulses and appropriate phase cycling [16].

(5) Phase control of individual states in a superposition is not as straightforward for quadrupole nuclei as for spin-1/2 systems.

(6) Relaxation is much faster in spin-3/2 systems than in its spin-1/2 counterpart.

The last two items of the above list can explain the almost complete absence in the literature of implementations of full algorithms in these systems (see, however, Refs. [17,18]). To the best of our knowledge, none of these aspects has been systematically studied in quadrupole systems.

The Hamiltonian, given in Eq. (1), is assumed to be static, but fluctuations in time occur in both magnetic and electric contributions. They lead to relaxation and then to loss of coherence. Therefore, it is important to investigate relaxation in the context of NMR quantum computing. In this paper, we study some NMR gate states and their relaxation in the two-

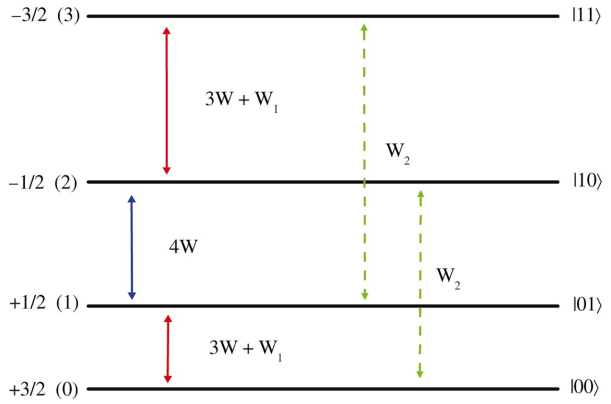

FIG. 1. (Color) Logical labeling of levels and relaxation rates for $I=3/2$ nuclei, according to Ref. [19]. W is the first-order magnetic contribution; W_1 and W_2 are, respectively, first- and second-order electric quadrupolar contributions. The deviations of populations from equillibrium between adjacent levels are represented by N_1, N_2, and N_3 (see text).

qubit system represented by ^{23}Na nuclei in a lyotropic liquid crystal at room temperature. Specifically, the preparation and time evolution of the pseudopure states, labeled as $|00\rangle$, $|01\rangle$, $|10\rangle$, $|11\rangle$, and Hadamard states (states created after application of a Hadamard gate) $|00\rangle+|01\rangle$ and $|10\rangle+|11\rangle$, and simulated pseudo-Bell states $|01\rangle+|10\rangle$ and $|00\rangle+|11\rangle$ have been investigated. Individual state phase control is verified in the case of superpositions by applying the respective ''reading'' operator and comparing the resulting state to the original pseudopure one.

Results of spin-lattice relaxation are analyzed according to the model of Suter *et al.* [19], solving the master equation, which takes into account mixed magnetic dipole and electric quadrupole contributions. In this model, the deviation of the population difference from its equilibrium value, at an instant t, for a spin $I=3/2$, follows a multiexponential law:

$$N_j(t)=\Delta_j^{eq}+\sum_{i=1,2,3} a_i e^{\lambda_i t}, \quad j=1,2,3, \tag{2}$$

where a_i and λ_i are both functions of three decay parameters: (i) W—first-order magnetic dipolar ($\Delta m=\pm 1$); (ii) W_1—first-order electric quadrupolar ($\Delta m=\pm 1$), and (iii) W_2—second-order electric quadrupolar ($\Delta m=\pm 2$). The λ_i coefficients are the eigenvalues of the relaxation matrix [19], given by

$$\lambda=\begin{bmatrix} -(7W+W_1+W_2)+\beta \\ -[6W+2(W_1+W_2)] \\ -(7W+W_1+W_2)-\beta \end{bmatrix}, \tag{3}$$

where $\beta=\sqrt{(W_1-W_2)^2+6W(W_1-W_2)+25W^2}$. The a_i coefficients are also functions of the initial distribution of populations, as it is described in the Appendix. The elements of Δ^{eq} are the populations differences, between adjacent levels, at the equilibrium. They are taken as zero in Ref. [19], but in the ideal case described in Ref. [11] they are given by $\Delta^{eq}=[1,1,1]$. In Fig. 1, the level scheme, state labels, and relaxation rate parameters for $I=3/2$ are shown.

II. SELECTIVE NMR QUANTUM GATES

The basic pulse sequences for generating pseudopure states in a $I=3/2$ quadrupole system are given in Ref. [11]. An interesting alternative using double-quantum pulses is given in Ref. [17]. In the present work, the *phase* of pulses which generate the Controlled-NOT (CNOT) gate is modified with respect to the proposal of Ref. [11]. Following the notation introduced in that reference, our sequence is

$$\mathrm{XOR_A}=(\pi)_{12}^{y}-(\pi)_{23}^{y}-(\pi)_{12}^{x},$$

where time is ordered from left to right. This modification is essential for creating coherent states. Here $(\pi)_{12}^{y}$ represents a rf pulse applied in the y direction, tuned to the 12 transition (see Fig. 1).

The Hadamard sequence applied over qubit A is the same as that built by Chuang *et al.* [4] for spins 1/2, the only difference being that in the present case the pulses are selective:

$$\mathrm{HD_A}=(\pi/2)_{01}^{y}-(\pi)_{01}^{-x}.$$

Ignoring global phases and normalization factors, the sequence above takes $|00\rangle$ to $|00\rangle+|01\rangle$ *and* $|01\rangle$ to $|00\rangle-|01\rangle$. This property is very important because it makes Hadamard self-inverse: $\mathrm{HD_A^2}|00\rangle=|00\rangle$. The sequence that takes $|10\rangle$ to $|10\rangle+|11\rangle$ and $|11\rangle$ to $|10\rangle-|11\rangle$ is similar to the above one, the only difference being on the selectivity of the transition.

The combination of CNOT and Hadamard gates acts as a macroscopic quantum superposition (cat state) generator [20] operator

$$G_{cat}=\underbrace{(\pi/2)_{01}^{y}-(\pi)_{01}^{-x}}_{\mathrm{HD}_A}-\underbrace{(\pi)_{12}^{y}-(\pi)_{23}^{y}-(\pi)_{12}^{x}}_{\mathrm{XOR}_A}.$$

G_{cat} takes $|00\rangle$ to $|00\rangle+|11\rangle$. One interesting variation of this sequence is the use of a double-quantum pulse between the levels 1 and 3, in place of the last three pulses [10]

$$G_{cat}^{DQ}=(\pi/2)_{01}^{y}-(\pi)_{01}^{-x}-(\pi)_{13}^{x}.$$

The main advantage of using double-quantum pulses is making the sequences shorter, therefore reducing the spin-lattice relaxation effects and saving processing time.

The simulated pseudo-Bell state $|01\rangle+|10\rangle$ can be generated by the simpler sequence

$$(\pi)_{12}^{-x}-(\pi/2)_{12}^{y},$$

which resembles a Hadamard sequence on the transition $1\leftrightarrow 2$. It is worth noticing that a single $\pi/2$ pulse on the same transition does not act in the same way as this operator, although both act upon level populations in the same way.

III. EXPERIMENT

^{23}Na NMR experiments were performed using a 9.4 T-VARIAN INOVA spectrometer in a lyotropic liquid-

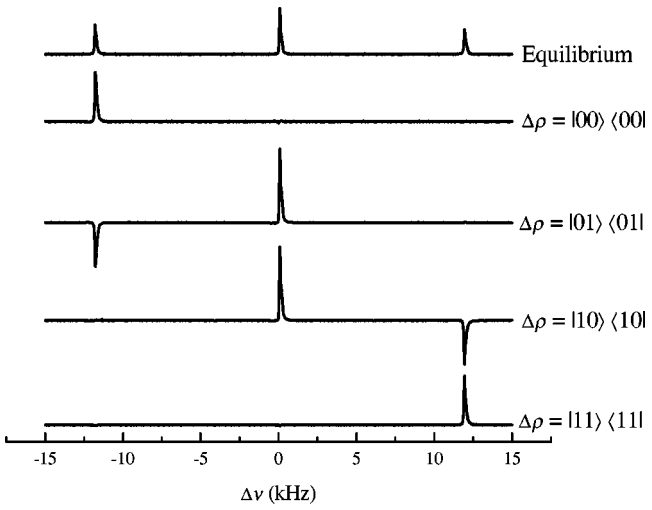

FIG. 2. Equilibrium and pseudopure NMR spectra of ^{23}Na. Quadrupole splitting is about 11 kHz. $\Delta\rho$ stands for ''deviation-from-unit'' density matrix [20].

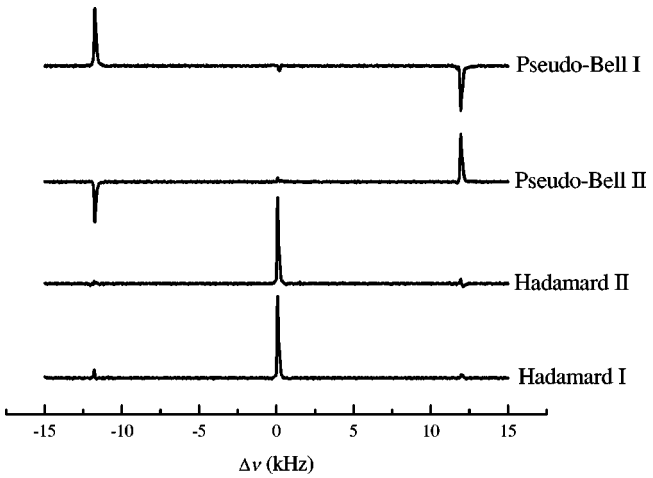

FIG. 3. Hadamard and pseudo-Bell state NMR spectra. Hadamard-I corresponds to the state $|00\rangle+|01\rangle$ and Hadamard-II corresponds to $|10\rangle+|11\rangle$. The pseudo-Bell states are pseudo-Bell I $|01\rangle+|10\rangle$ and II $|00\rangle+|11\rangle$. Although the two Hadamard spectra look the same, they correspond to different density matrices.

crystal system prepared with 35.9 wt. % of sodium decyl sulfate (Fluka), 7.2 wt. % decanol (Supelco), and 56.9 wt. % of deuterium oxide (D_2O, Merck), following the procedure described elsewhere [21].

^{23}Na NMR data were recorded at room temperature using a home-built single-resonance probe with radio-frequency (rf) Helmholtz-like rectangular coils (only one loop 2.5 cm high and 1 cm wide) separated by 7.5 mm. The geometry of the coils was chosen in order to improve rf magnetic-field homogeneity along the sample, which was packed in a 5-mm NMR tube 0.5 cm high.

In order to keep the pulse sequences as short as possible to reduce spin-lattice relaxation effects during the creation of pseudopure states and implementation of logic gates, 400 ms selective Gaussian shaped, single-quantum rf pulses were used to perform saturation ($\pi/2$) and inversion (π) of populations between adjacent levels. The mean rf amplitudes were adjusted to satisfy the selectivity condition [14,22,23]. The ratios were chosen to be ≈ 0.1 and 0.2 for the selective $\pi/2$ and π pulses, respectively, which guarantee their selectivities. The pulse selectivities were carefully calibrated by applying the selective saturation and inversion pulses to each line separately. The frequency offset was also optimized to improve the selectivity. Double-quantum selective pulse technique was also employed, following Ref. [17].

A nonselective hard pulse of $\pi/20$ 1.5 μs long was applied in order to measure the differences of populations for the three pairs of neighboring levels. The CYCLOPS phase cycling scheme was used to eliminate undesired transversal coherences, instead of using magnetic-field gradients [10,16]. Experiments were performed with a recycle delay of 500 ms.

IV. RESULTS

In Fig. 2 it is shown the NMR spectra for equilibrium and pseudopure states, generated with double-quantum technique. The main difference between our spectra and the results of Ref. [11] is in the magnitude of the quadrupolar splitting, which is much bigger in our case (≈ 11 kHz, compared to ≈ 1.1 kHz). Figure 3 exhibits the four spectra corresponding to the superposition states studied in this work. The coherences of Hadamard and pseudo-Bell II states were checked by applying the respective logical pulse sequences twice and measuring the degree of recovery of the original pseudopure state. Pseudo-Bell I state was checked applying the sequence in reversed order, that is, first the CNOT and then the HDA gates. In the case of both Hadamard states, the recovery reached 80% of the initial state, whereas in the case of the pseudocat state it was about 65% only. In the case of the second pseudo-Bell state, the recovery was over 90%. Failure to fully recover the states can be ascribed to small imperfections in rf pulses and relaxation effects. It is interesting to note that although the two Hadamard spectra have the same appearance, one must remember that first-order coherences are different in the two respective density matrices. This is a good example of how density matrices carry more information than NMR spectra themselves [24].

Figure 4 exhibits spin-lattice relaxation curves for each line of the NMR spectrum for the four pseudopure states and Figure 5 shows the same study for the coherent states shown in Fig. 3. Continuous lines are calculated curves following the model of Suter *et al.* [19], Eq. (2). From these curves, we established the following values for the individual relaxation rates:

$$W = 13.8 \pm 0.8 \ \mathrm{s}^{-1},$$

$$W_1 = 24.6 \pm 1.5 \ \mathrm{s}^{-1},$$

$$W_2 = 2.3 \pm 0.5 \ \mathrm{s}^{-1},$$

and consequently, to the relaxation matrix eigenvalues [19]

$$\lambda_1 = -39 \pm 4 \ \mathrm{s}^{-1},$$

$$\lambda_2 = -137 \pm 9 \ \mathrm{s}^{-1},$$

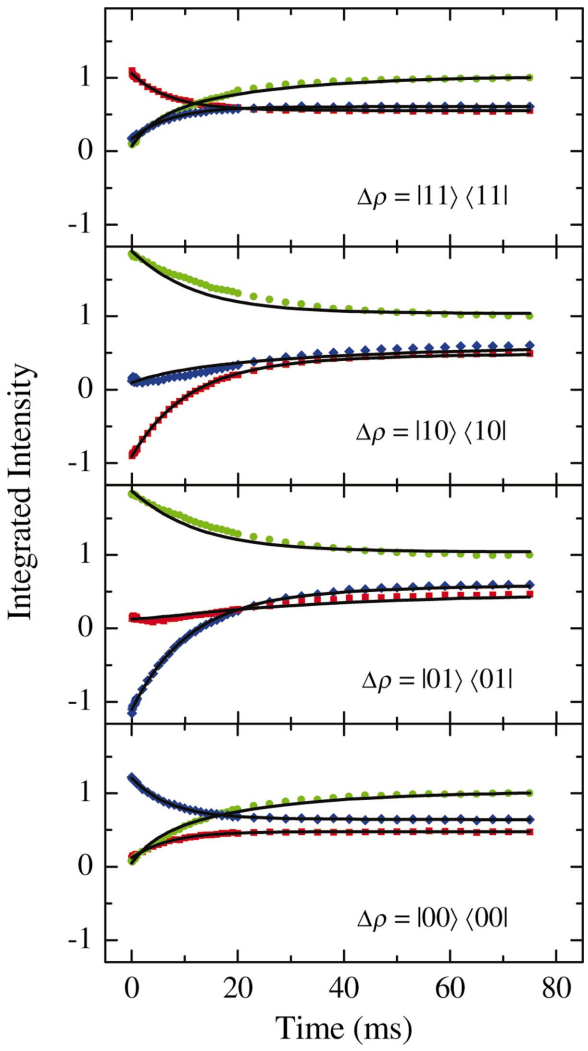

FIG. 4. (Color) Relaxation of pseudopure states. Symbols: "squares" (red), transition $|00\rangle \leftrightarrow |01\rangle$; "circles" (green), transition $|01\rangle \leftrightarrow |10\rangle$, and "diamonds" (blue), transition $|10\rangle \leftrightarrow |11\rangle$. The continuous line is the calculation using the model of Suter *et al.* [19].

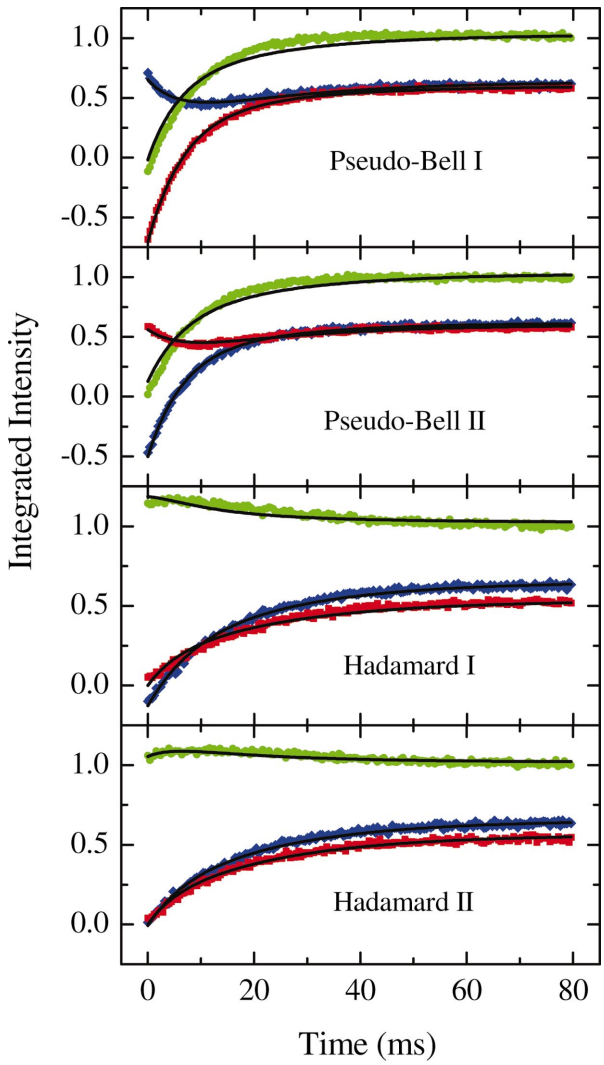

FIG. 5. (Color) Relaxation of superposition states. Symbols: "squares" (red), transition $|00\rangle \leftrightarrow |01\rangle$; "circles" (green), transition $|01\rangle \leftrightarrow |10\rangle$; and "diamonds" (blue), transition $|10\rangle \leftrightarrow |11\rangle$. Continuous line is the calculation using the model of Suter *et al.* [19].

$$\lambda_3 = -208 \pm 12 \ \ \mathrm{s}^{-1},$$

These numbers are in general agreement with other relaxation studies [25] made in ^{23}Na as well as in other quadrupolar nuclei [26–28]. In order to compare these numbers with the ones obtained through the usual procedure of single growing exponential fit, we performed selective inversion recovery on the three transitions. The results yielded $1/T_1 \approx 66.8\ \mathrm{s}^{-1}$, for the central transition, and $1/T_1 \approx 89.2\ \mathrm{s}^{-1}$, for both satellites. If we were to consider the central line relaxation governed by a single exponential [12], one would have obtained $1/T_1 = 2 \times 4W \approx 110\ \mathrm{s}^{-1}$.

According to Suter *et al.*, not only are the relaxation rates functions of the W's, but also the *amplitudes* of the exponentials, the a_i coefficients. In the Appendix, we list some of the amplitudes calculated for the ideal situation described in Refs. [10,11] and compare to coefficients obtained from the *experimental* initial distributions. This was done by taking the differences in amplitudes of each relaxation curve at $t = 0$ and at the saturation, as the deviation of the population difference. We can notice the fairly good agreement between signs and magnitudes of the coefficients. The discrepancy in the initial conditions is in magnitude, but the correlation in sign is excellent. These differences affect the relaxation coefficients and therefore the shape of the relaxation curves, but not spectral data used to interpret the execution of the quantum logic gates.

V. CONCLUSIONS

In this paper, we presented a detailed study of relaxation of coherent states in the two-qubit quantum computing system represented by ^{23}Na nuclei in a lyotropic liquid crystal. The coherence of states was verified by applying the corresponding selective logic gates, followed by the respective reading gate, and the result compared to the original pseudopure states. In all cases, a high degree of recovery was

achieved, demonstrating the coherent action of each gate. Coherences are maintained for times comparable to transverse relaxation time T_2, around 4 ms in the system studied (measured on the central line transition). T_2 was found to be independent of level populations.

We found that spin-lattice relaxation of coherent states is in good agreement with a model where mixed, magnetic dipole, and electric quadrupole terms contribute simultaneously to every transition. Individual relaxation rates cannot be, in general, experimentally discriminated. Relaxation coefficients were calculated, following Ref. [19], from experimental data and compared to ideal expressions. It is worth mentioning that the longitudinal relaxation times T_1 obtained from fitting single growing exponentials to the pseudopure states are not related in a simple way to the values that were determined using the model [19].

Execution of gates and algorithms in NMR quantum computing rely on the production of coherent states, and therefore depend on the knowledge of relaxation. If on one hand, implementation of gates depend on the control of static Hamiltonian terms, relaxation is caused by *fluctuations* in the interaction terms. These fluctuations are at the core of the debate whether NMR is capable or not of performing true quantum computing [1], and relate to loss of coherence of quantum states. The interpretation of NMR spectra resulting from quantum logical operations, on its turn, depends on the distribution of Zeeman level populations. The present study showed that deviations between the ideal and real distributions affect relaxation, but not quantum gate implementations.

Finally, it is worth mentioning a possible application of the present analysis outside the strict domain of quantum computing. The techniques developed for the construction of quantum logic gates allow the creation of very particular initial conditions, from which the relaxation dynamics can be followed and analyzed in the framework of mixed quadrupolar and magnetic interactions. The possibility of preparation of very specific initial states, exemplified in this work by the preparation of pseudopure, pseudo-Bell, and Hadamard states, offers a powerful tool for analyzing relaxation data, as the dynamics of the spin-lattice relaxation of quadrupolar nuclei is critically dependent on the initial conditions. This can be useful for identifying relaxation mechanisms and extracting relaxation parameters in the analysis of relaxation of quadrupolar nuclei in solid or liquid-crystal materials.

ACKNOWLEDGMENTS

The authors acknowledge support from CAPES, CNPq, and FAPESP. R.S.S. especially acknowledges the Brazilian Quantum Information (CNPq) project and the CAPES Prodoc grant program.

APPENDIX: IDEAL AND EXPERIMENTAL RELAXATION A_i COEFFICIENTS CALCULATED FOR SOME NMR COHERENT STATES

Preliminary definitions and explanations are as follows:

(i) $\beta=\sqrt{(W_1-W_2)^2+6W(W_1-W_2)+25W^2}$,

(ii) N_0 is the ideal initial deviation of the population difference from its equilibrium value [19].

(iii) N_0^{expt} is the experimental initial deviation of the population difference from its equilibrium value.

(iv) The number in parentheses in a_{2s} refers to the higher-energy satellite.

1. Pseudopure states

(a) $|00\rangle - N_0=[1,-1,-1]$; $N_0^{expt}=[0.542,-0.901,-0.430]$,

$$a_{1c}=-\frac{W-W_1+W_2-\beta}{2\beta},$$

$$a_{1c}^{expt}=-\left(0.888+0.014\frac{W_1-W_2-\beta}{W}\right)\left(\frac{W-W_1+W_2-\beta}{2\beta}\right),$$

$$a_{2c}=0, \quad a_{2c}^{expt}=0,$$

$$a_{3c}=\frac{W-W_1+W_2+\beta}{2\beta},$$

$$a_{3c}^{expt}=\left(0.888+0.014\frac{W_1-W_2+\beta}{W}\right)\left(\frac{W-W_1+W_2+\beta}{2\beta}\right),$$

$$a_{1s}=2\frac{W}{\beta},$$

$$a_{1s}^{expt}=1.77\frac{W}{\beta}+0.028\frac{W_1-W_2-\beta}{\beta},$$

$$a_{2s}=-1(+1), \quad a_{2s}^{expt}=-0.49(+0.49),$$

$$a_{3s}=-2\frac{W}{\beta},$$

$$a_{3s}^{expt}=-1.77\frac{W}{\beta}-0.028\frac{W_1-W_2+\beta}{\beta}.$$

(b) $|01\rangle - N_0=[-3,1,-1]$, $N_0^{expt}=[-1.749,0.833,-0.333]$,

$$a_{1c}=\frac{(W+W_1-W_2-\beta)(W-W_1+W_2-\beta)}{4W\beta},$$

$$a_{1c}^{expt}=\frac{[1.145W+0.521(W_1-W_2-\beta)](W-W_1+W_2-\beta)}{4W\beta},$$

$$a_{2c}=0, \quad a_{2c}^{expt}=0,$$

$$a_{3c}=-\frac{(W+W_1-W_2+\beta)(W-W_1+W_2+\beta)}{4W\beta},$$

$$a_{3c}^{expt} = -\frac{[1.145W+0.521(W_1-W_2+\beta)](W-W_1+W_2+\beta)}{4W\beta},$$

$$a_{1s}=-\frac{W+W_1-W_2-\beta}{\beta},$$

$$a_{1s}^{expt}=-\frac{1.145W+0.521(W_1-W_2-\beta)}{\beta},$$

$$a_{2s}=+1(-1), \quad a_{2s}^{expt}=+0.708(-0.708),$$

$$a_{3s}=\frac{W+W_1-W_2+\beta}{\beta},$$

$$a_{3s}^{expt}=\frac{1.145W+0.521(W_1-W_2+\beta)}{\beta}.$$

2. Hadamard states

$|00\rangle+|01\rangle-N_0=[-1,0,-1], \quad N_0^{expt}=[-0.733,0.145,-0.465],$

$$a_{1c}=-\frac{(W-W_1+W_2+\beta)(W-W_1+W_2-\beta)}{8W\beta},$$

$$a_{1c}^{exp} = -\frac{[0.020W+0.599(-W_1+W_2+\beta)](W-W_1+W_2-\beta)}{8W\beta},$$

$$a_{2c}=0, \quad a_{3c}^{expt}=0,$$

$$a_{3c}=+\frac{(W-W_1+W_2+\beta)(W-W_1+W_2-\beta)}{8W\beta},$$

$$a_{3c}^{expt} = \frac{[0.020W+0.599(-W_1+W_2+\beta)](W-W_1+W_2-\beta)}{8W\beta},$$

$$a_{1s}=\frac{W-W_1+W_2+\beta}{2\beta},$$

$$a_{1s}^{expt}=\frac{0.020W+0.600(-W_1+W_2+\beta)}{2\beta},$$

$$a_{2s}=0, \quad a_{2s}^{expt}=+0.134(-0.134),$$

$$a_{3s}=-\frac{W-W_1+W_2-\beta}{2\beta},$$

$$a_{3s}^{expt}=-\frac{0.020W+0.600(-W_1+W_2+\beta)}{2\beta}.$$

3. Pseudo-cat state

$|00\rangle+|11\rangle-N_0=[0,-1,-2], \quad N_0^{expt}=[0.092,-1.115,-1.265],$

$$a_{1c}=-\frac{(5W-W_1+W_2+\beta)(W-W_1+W_2-\beta)}{8W\beta},$$

$$a_{1c}^{expt} = -\frac{[5.046W+0.587(-W_1+W_2+\beta)](W-W_1+W_2-\beta)}{8W\beta},$$

$$a_{2c}=0, \quad a_{2c}^{expt}=0,$$

$$a_{3c}=\frac{(5W-W_1+W_2-\beta)(W-W_1+W_2+\beta)}{8W\beta},$$

$$a_{3c}^{expt} = \frac{[5.046W+0.587(-W_1+W_2-\beta)](W-W_1+W_2+\beta)}{8W\beta},$$

$$a_{1s}=\frac{5W-W_1+W_2+\beta}{2\beta},$$

$$a_{1s}^{expt}=\frac{5.046W+0.587(-W_1+W_2+\beta)}{2\beta},$$

$$a_{2s}=-1(+1), \quad a_{2s}^{expt}=-0.678(+0.678),$$

$$a_{3s}=-\frac{5W-W_1+W_2-\beta}{2\beta},$$

$$a_{3s}^{expt}=-\frac{5.046W+0.587(-W_1+W_2-\beta)}{2\beta}.$$

[1] S.L. Braunstein, C.M. Caves, R. Jozsa, N. Linden, S. Popescu, and R. Schack, Phys. Rev. Lett. **83**, 1054 (1999); see also N. Linden and S. Popescu, *ibid.* **87**, 047901 (2001); see, however, R. Laflamme, http://quickreviews.org/cgi/display.cgi?reviewID=laf.q-p. 9 811 018; G.L. Long, H.Y. Yan, Y.S. Li, C.C. Tu, S.J. Zhu, D. Ruan, Y. Sun, J.X. Tao, and H.M. Chen, Commun. Theor. Phys. **38**, 305 (2002).

[2] N. Linden, H. Barjat, and R. Freeman, Chem. Phys. Lett. **296**, 61 (1998).

[3] J.A. Jones, M. Mosca, and R.H. Hansen, Nature (London) **393**, 344 (1998).

[4] I.L. Chuang, N. Gershenfeld, and M. Kubinec, Phys. Rev. Lett. **80**, 3408 (1998).

[5] L.M.K. Vandersypen, M. Steffen, G. Breyta, C.S. Yannoni,

M.H. Sherwood, and I.L. Chuang, Nature (London) **414**, 883 (2001).
[6] M.A. Nielsen, E. Knill, and R. Laflamme, Nature (London) **396**, 52 (1998).
[7] A.K. Khitrin and B.M. Fung, Phys. Rev. A **64**, 032306 (2001).
[8] C.H. Tseng, S. Somaroo, Y. Sharf, E. Knill, R. Laflamme, T.F. Havel, and D.G. Cory, Phys. Rev. A **61**, 012302 (1999).
[9] E. Knill, R. Laflamme, R. Martinez, and C.-H. Tseng, Nature (London) **404**, 368 (2000).
[10] A.K. Khitrin and B.M. Fung, J. Chem. Phys. **112**, 6963 (2000).
[11] N. Sinha, T.S. Mahesh, K.V. Ramanathan, and A. Kumar, J. Chem. Phys. **114**, 4415 (2001).
[12] *Principles of Magnetic Resonance*, edited by C. P. Slichter, 3rd ed. (Springer-Verlag, Berlin, 1990).
[13] P.P. Man, J. Klinowski, A. Trokiner, H. Zanni, and P. Papon, Chem. Phys. Lett. **151**, 143 (1988).
[14] S. Vega, J. Chem. Phys. **68**, 5518 (1978).
[15] J.A. Jones, Prog. Nucl. Magn. Reson. Spectrosc. **38**, 325 (2001).
[16] A.K. Khitrin, H. Sun, and B.M. Fung, Phys. Rev. A **63**, 020301 (2001).
[17] V.L. Ermakov and B.M. Fung, Phys. Rev. A **66**, 042310 (2002).
[18] K.V.R.M. Murali, N. Sinha, T.S. Mahesh, M.H. Levitt, K.V. Ramanathan, and A. Kumar, Phys. Rev. A **66**, 022313 (2002).
[19] A. Suter, M. Mali, J. Ross, and D. Brinkmann, J. Phys.: Condens. Matter **10**, 5977 (1998).
[20] *Quantum Computation and Quantum Information*, edited by M.A. Nielsen and I.L. Chuang (Cambridge University Press, Cambridge, 2002).
[21] K. Radley, L.W. Reeves, and A.S. Tracey, J. Phys. Chem. **80**, 174 (1976).
[22] A. Wokaun and R.R. Ernst, Chem. Phys. Lett. **52**, 407 (1997).
[23] S. Vega and A. Pines, J. Chem. Phys. **66**, 5624 (1977).
[24] G.L. Long, H.Y. Yan, and Y. Sun, J. Opt. B: Quantum Semiclassical Opt. **3**, 376 (2001).
[25] P. Porion, M. Al Mukhtar, S. Meyer, A.M. Faugère, J.R.C. van der Maarel, and A. Delville, J. Phys. Chem. B **105**, 10 505 (2001).
[26] M. Holz, J. Mol. Liq. **67**, 175 (1995).
[27] R.P.W.J. Struis, J. de Bleijser, and J.C. Leyte, J. Phys. Chem. **93**, 7932 (1989).
[28] M. Odelius, M. Holz, and A. Laaksonen, J. Phys. Chem. A **101**, 9537 (1997).